Shear stiffness of GFRP-reinforced concrete squat wall under seismic loading

Ahmed Arafa[1], Ahmed Farghaly[2], Brahim Benmokrane[3]

[1] Ph.D. Student, Department of Civil Engineering, University of Sherbrooke - Sherbrooke, QC, Canada.
[2] Research Associate, Department of Civil Engineering, University of Sherbrooke - Sherbrooke, QC, Canada
[3] Professor, Department of Civil Engineering, University of Sherbrooke - Sherbrooke, QC, Canada.

ABSTRACT

Experimental test results on the behavior of squat walls entirely reinforced with glass fiber-reinforced polymer (GFRP) reinforcement have demonstrated the feasibility of such structural element in using as a lateral seismic resistance element in low-to-moderate earthquake regions. The findings also strongly suggested proposing design guidelines for such structural elements. This study aimed at evaluation the walls' shear stiffness. Based on the test results, the variation of shear deformations with top displacements was discussed. Based on regression analyses of test results, expressions that are directly correlated the lateral shear stiffness with lateral drift was generated.

Keywords: squat wall, GFRP bars, shear stiffness.

INTRODUCTION

The use of fiber-reinforced polymer (FRP) composite materials has been growing in efforts to counter deterioration resulting from the corrosion of steel reinforcement, covering construction elements such as columns, beams and slabs. However, since these investigations mainly focused on the behavior under static-loading conditions omitting the seismic design; the feasibility of using FRP as internal reinforcement for a complete structure that combines such elements while having the stiffness, and deformation capacity to resist seismic loads, has become questionable. To address this issue, an experimental study on the behavior of mid-rise walls has been conducted [1]. The test results demonstrated the potential of GFRP reinforcement in distribution the shear deformations along the wall height, owing to its elastic nature, resulting in control shear distortion relatively to that in the steel-reinforced wall in which shear distortion took place simultaneously with flexural reinforcement yielding and mobilized at the plastic hinge zone causing deterioration of shear resistance.

The test results conducted in GFRP-reinforced mid-rise walls in term of control shear deformations paved the way for a new experimental study to evaluate the feasibility of using GFRP bars in squat walls (having a shear span to length ratios less than 2.0) in which such problems are frequently be encountered [2]. Arafa et al. [3] reported experimental results on two squat walls: one was reinforced with conventional steel bars, while the second was reinforced with GFRP bars. The GFRP-reinforced squat wall attained satisfactory strength and stable cyclic behavior as well as self-centering ability that assisted in avoiding sliding shear, which occurred in the companion steel-reinforced one.

This paper focuses mainly on estimation the shears stiffness of GFRP-reinforced squat walls as a lateral seismic element. Shear deformations' variation with top displacements were conducted and discussed, with showing the difference of deformation characteristics between GFRP and steel-reinforced squat walls. Evaluation of the shear stiffness for the tested GFRP-reinforced walls using expressions that are being used in steel-reinforced walls; owing to the absence of formula for FRP-reinforced elements, taking into account the difference of mechanical characteristics between steel and FRP reinforcement is then discussed and compared to experimental result.

SUMMARY OF EXPERIMENTAL PROGRAM AND RESULTS

Five full-scale reinforced-concrete squat walls were constructed and tested to failure under quasi-static reversed cyclic lateral loading. Four specimens were entirely reinforced with GFRP bars (G4-250, G4-160, G4-80, and G6-80) and one was reinforced with steel bars (S4-80). Figure 1 shows the concrete dimensions, reinforcement configuration, and the test setup. The boundary elements' longitudinal- and transverse-reinforcement ratios and vertical web reinforcement were 1.43%, 0.89%, and 0.59%, respectively, in all specimens. Four horizontal web reinforcement ratios equal to 0.51%, 0.79%, 1.58%, and 3.58% were used in G4-250, G4-160, G4-80, and G6-80 with #4 GFRP bars spaced at 250, 160, and 80 mm or #6 GFRP bars spaced at 80 mm, respectively. Specimen S4-80 served as a reference for G4-80, so both specimens had identical reinforcement configurations

and ratios. Bidiagonal #3 GFRP bars were added to prevent sliding shear. Figures 1c and 1d show the test setup and loading history, respectively. Table 1 provides the mechanical properties of the reinforcement.
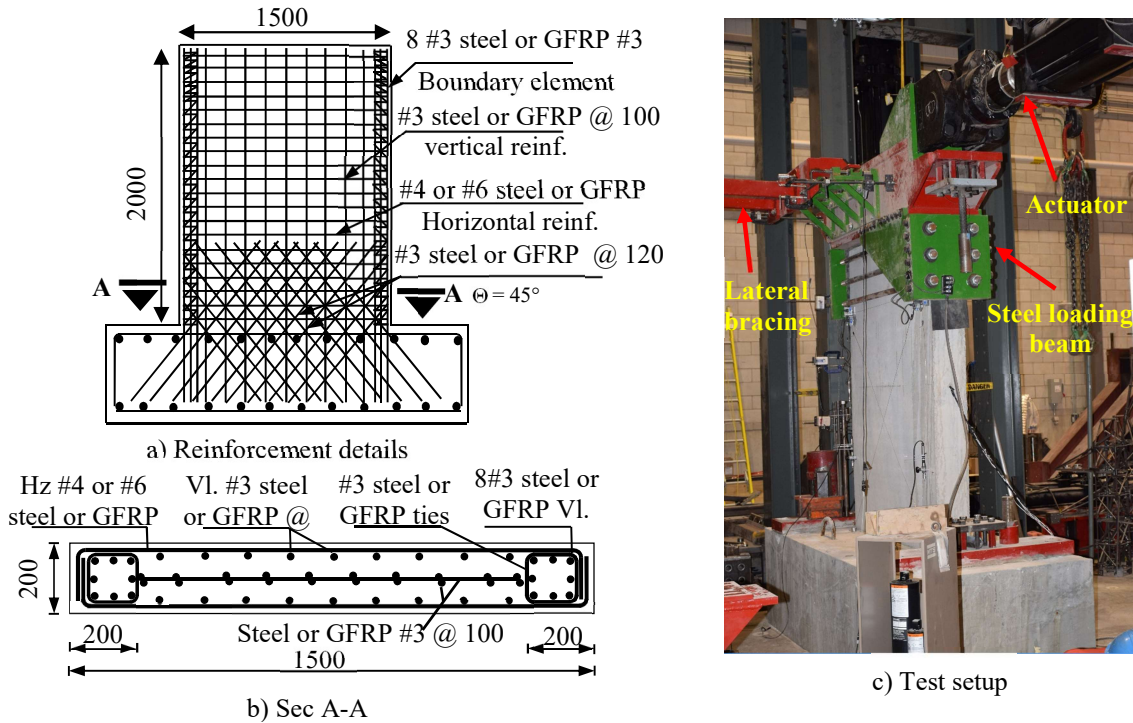

a) Reinforcement details

b) Sec A-A

c) Test setup

Figure 1. Concrete dimensions, reinforcement details, and test setup.

Table 1. Tensile properties of the reinforcement

Bar	Designated Bar Diameter (mm)	Nominal Area[1] (mm²)	Tensile Modulus of Elasticity (GPa)	Tensile Strength[2]* (MPa)	Average Strain at Ultimate (%)
Straight bars					
#3 GFRP	9.5	71	65	1372	2.1
#3 steel	9.5	71	200	$f_y = 420$	$\varepsilon_y = 0.2$
#4 steel	12.7	129	200	$f_y = 420$	$\varepsilon_y = 0.2$
Bent #3 GFRP – rectilinear spiral					
Straight	9.5	71	50	1065	2.1
Bent			---	460	---
Bent #4 GFRP – horizontal bar					
Straight	12.7	129	50	1020	2.0
Bent			---	459	---
Bent #6 GFRP – horizontal bar					
Straight	19.1	285	50	1028	2.0
Bent			---	463	---

f_y: steel yielding strength, ε_y: steel yielding strain.
[1]According to CSA S807 (CSA, 2010)
[2] Tensile properties were calculated using nominal cross-sectional areas.
*Guaranteed tensile strength: Average value – 3 × standard deviation (ACI 440.1R-15)

Figure 2 shows typical modes of failure that observed through testing. Specimen S4-80 exhibited premature sliding shear failure (Figure 2a) due to yielding of flexural reinforcement that caused formation of a major continuous flexural crack along the end line of the bi-diagonal sliding reinforcement, along which sliding shear deformations commenced and gradually dominated the behavior. Such behavior; however, was prevented in its counterpart specimen G4-80 that exhibited flexural compression failure with no sign of premature sliding or anchorage failure (Figure 2b). This was attributed to the elastic nature of GFRP bars that assisted the cracks to realign and lock up in compression zone as well as distributing shear deformations along the wall height rather than localization at plastic hinge zone. The envelop curves for the load-top lateral displacement is plotted in Figure 3. As shown, both specimens exhibited similar initial stiffness; however, owing to the low elastic modulus of the used GFRP bars,

G4-80 experienced softer behavior than S4-80 after the first flexural crack initiation. This behavior kept constant up to a lateral drift of 1.35% (the intersection between two envelop) corresponding to 99% and 56% of ultimate load for SX4 and GX4, respectively. Thereafter, the strength of S4-80 deteriorated due to the localized sliding shear deformations, while G4-80's strength kept increasing almost proportionally with load increase to achieve ultimate load and drift capacity higher than SX4, with ratios equal to 71% and 50%, respectively. Overall, the observed behavior reveals the acceptable behavior of GFRP-reinforced walls as a lateral resisting system in low to moderate earthquake regions. In regions prone to strong earthquake; however, merging steel with FRP reinforcement would be more effective solution. In such case, FRP reinforcement will control the permanent deformations of the structure beyond an earthquake as well as prevent the premature sliding failure while steel reinforcement will provide the structure with ductility and consequently reduction in the seismic demand.

The failure of G6-80 was identified as flexural compression failure as shown in Figure 2c; similarly to its counterpart G4-80. However, the rest two specimens experienced two different mode of failure; the failure of G4-250 occurred by sliding along a major diagonal shear crack (Figure 2d) due to the inadequacy of horizontal web reinforcement while G4-160 experienced sudden flexural rupture in the longitudinal bars at the boundary element under tension (Figure 2e). Referring to Figure 3 that show the load-top later displacement envelop curves for the test specimens, it is clear that horizontal web reinforcement ratio has a significant effect in increasing the ultimate strength and drift ratio; however, this effect appears to be insignificant if the wall was provided with horizontal web reinforcement higher than that required for flexural resistance (G6-80 compared to G4-80).
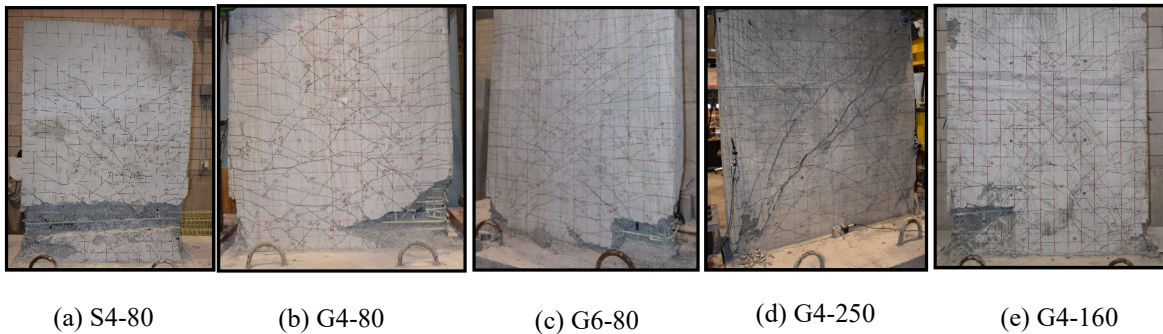

(a) S4-80　　　(b) G4-80　　　(c) G6-80　　　(d) G4-250　　　(e) G4-160

Figure 2. Failure modes of test specimens; (a) sliding shear, (b) and (c) flexural compression, (d) diagonal tension shear and (e) flexural tension.
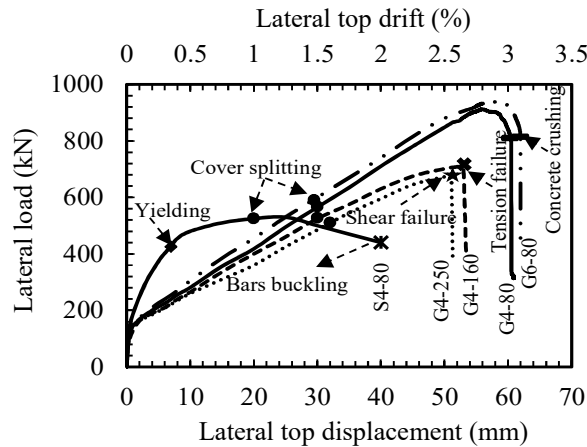

Figure 3. Load-top displacement envelop curves.

FLEXURE AND SHEAR DEFORMATIONS

Generally, the total lateral displacement of a cantilever squat wall under seismic loading can be characterized into three fundamental components: (1) flexural displacement Δf, (2) shear displacement of the web , Δs, which can result from the activation of two individual types of deformations: the shear deformations caused by diagonal tension and any deformations caused by sliding shear in the web zone (such as the case of S4-80), and (3) sliding displacement Δsl along the joint between the wall and base. In the present study, the measured sliding displacements between the walls and foundation are relatively

small (the measured values during testing never exceeded 1%) and their contribution to the total displacement therefore will be omitted in the following discussion.

Early method for decoupling flexural and shear deformations by Osterle et al. [4] suggested that the shear deformation of a shear panel can be directly estimated from the changes in the length of the two diagonals using Eq. (1a) (with the model shown in Fig. 4a).

$$U_{s\ original} = \gamma_{original}\ h = \frac{(d_1^{/} - d)d - (d_2^{/} - d)d}{2hL} \tag{1a}$$

where $\gamma_{original}$ is the shear distortion over a height h, and are the lengths of the diagonal transducers after deformation, d is the original length of the diagonal before deformation, L, and h is respectively, the length and height of the panel at which the LVDTs are mounted. The flexural deformation, on the other hand, can be calculated from the elongation and the shortening of the two vertical LVDTs mounted at both boundaries with height h using Eq. (1b).

$$U_{f\ original} = \theta\ h = \frac{(V_L - V_R)}{L}\ h \tag{1b}$$

where θ is the rotation over the height h

a) Shear deformation

b) Flexural deformations, constant curvature along height

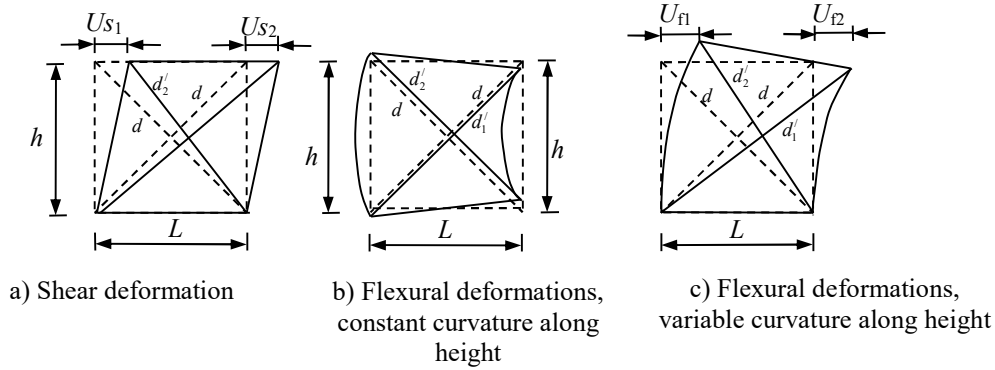c) Flexural deformations, variable curvature along height

Figure 4. Load-top displacement envelop curves.

Although using the foregoing method (Eq. 1a) have become very common way for estimating shear deformations in many test series, the deformation given by this method is overestimated because it contains flexural deformations as result of the variation of bending moment along the wall height. Hiraishi [5] demonstrated that this method is only valid if the center of rotation is located at the element center (i.e. constant curvature over the element height) accordingly, any change in diagonal lengths will be attributed to shear deformation and will not be affected by flexural deformation (Figure 4b). However, this is not the case of structural walls in which the curvature is not constant over the height due to moment variation; therefore, a portion of the change in diagonal lengths has to be attributed to flexural deformations (Figure 4c). In addition to the over estimation of shear deformation by using equation Eq. (1a), the calculated flexural deformation using Eq. (1b) may also lead to overestimated value as this equation is only valid if the curvature is concentrated at the wall base; i.e, the center of ration is located at the base, but this assumption might be incorrect in some cases owing to their dependency on many parameters such as the wall geometry, reinforcement type. Given the aforementioned shortcomings that stem mainly from the assumption of center of rotation's location, Hiraishi [5] suggested the following corrected equations that account for this parameter:

$$U_{s\ corrected} = U_{s\ original} - (\alpha - 0.5)\theta\ h$$
(2a)

$$U_{f\ corrected} = \alpha\theta\ h = \alpha\ U_{f\ original} \tag{2b}$$

$$\alpha = \frac{\int_0^h \theta(y)dy}{\theta h} \tag{2c}$$

The center of rotation (α) accounts for the variation in curvature along the panel height. Based on the measured rotation distribution along the wall height, the center of rotation was estimated and found to be 0.62 for S4-80, 0.59 for G6-80, and 0.58 for the other specimens.

SHEAR DEFORMATIONS CONTRIBUTION

Figure 5 plots of the corrected flexural and shear deformations. The behavior of all specimens was dominated initially by flexural response. With the initiation of the first shear crack, shear deformations began to participate in the total displacement. Clearly, the contribution of shear deformation varied as a function of reinforcement type (steel or GFRP) and horizontal web reinforcement ratio. In S4-80, the percentage of shear deformation to the total deformation corresponding to yielding of the longitudinal reinforcement was 22% (0.4% drift) and increased to 46% after the localization of sliding shear corresponding to concrete cover spalling (1.25% drift) and reached 64% at failure (2% drift). In the GFRP-reinforced specimens, the percentages were about 49%, 38%, 28%, and 15% for G4-250, G4-160, G4-80, and G6-80, respectively, up to 1% drift. At cover spalling (2% drift), the percentage increased slightly to 56%, 42%, 36%, and 20%, respectively, which remained almost constant up to failure. The results reveal that shear deformation should not be omitted, even if the shear strength was twice the applied load, as is the case with G6-80.
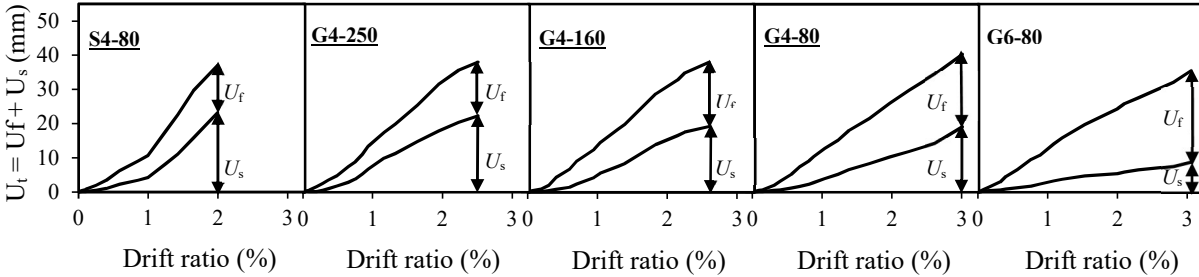

Figure 5. Displacement components at a height equal to the wall length.

Figures 6a and 6b show that, initial high shear stiffness was followed by a significant reduction in shear stiffness manifested with the appearance of the first shear crack. The figures underlines the link between steel yielding and shear deformations in S4-80, which exhibited significant degradation in shear stiffness after a few cycles of steel yielding associated with substantial increasing in shear deformation. In contrast, the shear deformation in GFRP-reinforced squat walls increased almost linearly with loading. The figures also reveal the effectiveness of the horizontal web reinforcement ratio in reducing shear deformation.
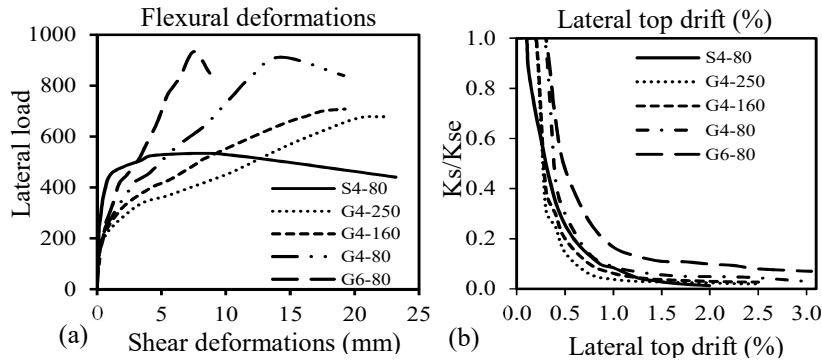

Figure 6. Comparison between shear deformations and stiffnesses for the test specimens.

PROPOSED MODEL FOR SHEAR STIFFNESS

Seismic design practice worldwide is moving toward displacement-based design method. This approach is basically concerned with the structure's effective properties at a targeted top drift level to achieve predefined performance level. Hence, it would be preferable, within the context of displacement-based design method, to develop a simple model that directly correlates the shear stiffness degradation of a wall to its top drift. In this regards, a methodology for prediction the normalized shear stiffness degradation based on regression analysis for the test results is conducted.

The results in Figure 7a generally reflects strong correlation between normalized shear stiffness and drift ratio ($R^2 = 0.87$). Interpretation of the results also revealed that normalized shear stiffness degradation is a function of horizontal web reinforcement ratio. As shown in Figure 7b, the degradation decreases almost linearly with increasing reinforcement ratio at the same drift level; however, the relation appears to significantly deviate with increasing drift level. This is clear from Figure 7c and d that show the non-linear variation of relation constants A and B with drift ratio; indicating the interrelation between drift ratio and horizontal web reinforcement ratio.
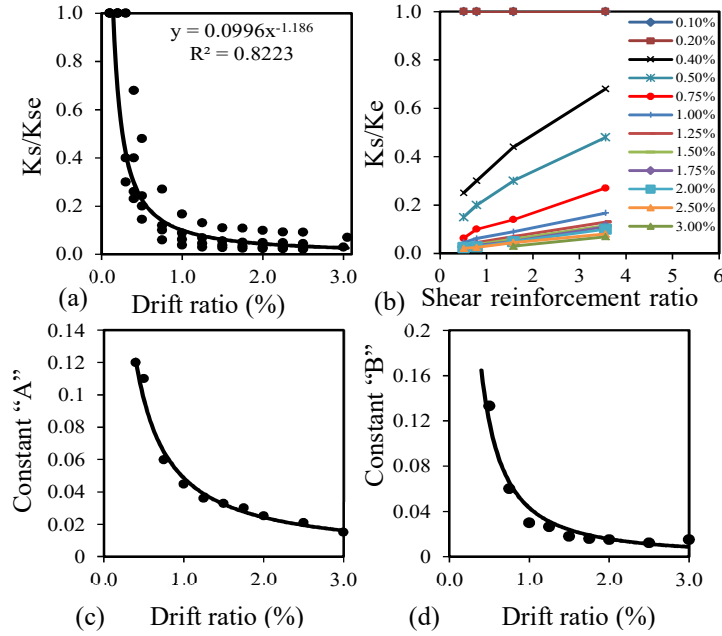
Figure 7. Validation of the proposed model for shear-stiffness degradation

Based on the aforementioned discussion, the normalized shear stiffness degradation is a function of top drift ratio and horizontal web reinforcement ratio and can be set in a form as follows:

$$\frac{K_s}{K_{se}} = a.\delta^x.\rho + b.\delta^y$$

(3)

where K_s is the secant shear stiffness at a lateral top drift equal δ, K_{se} is the elastic shear stiffness, ρ is the horizontal web reinforcement ratio, and a, b, x and y are the constants representing the correlation between each parameter and normalized shear stiffness. For our experimental data, the coefficients a, b, x and y that produce good match between experimental and analytical results were found equal to 0.04, 0.03, -1, and -1.6, respectively. Therefore, the normalized shear stiffness (K_s/K_{se}) can be rewritten as follows (SI units):

$$\frac{K_s}{K_{se}} = \frac{0.04\rho}{\delta} + \frac{0.03}{\delta^{1.6}}$$

(4)

CONCLUSIONS

The main purpose of this research was to evaluate the shear stiffness of squat walls reinforced with GFRP bars. The flexural and shear deformation was decoupled. It was shown that omitting the effect of curvature variation in decoupling resulted in significant overestimated deformations. Correcting the deformations; however, using the estimated center of rotation produced more consistent results. Contribution of each deformation mode to the total deformations showed the necessary of evaluating the cracked shear stiffness beside flexural stiffness. Within the context of displacement-based design method, a simple model that directly correlates the shear stiffness degradation of the test walls to their top drift was proposed.

AKNOWLEDGMENT

REFERENCES

[1] Mohamed, N., Farghaly, A. S., Benmokrane, B., and Neale, K. W., "Flexure and Shear Deformation of GFRP-Reinforced Shear Walls." Journal of Composites for Constructions, V. 18, No. 2, 2014b, 04013044.

[2] Luna, B. N., Rivera, J. P., and Whittaker, A. S., "Seismic Behavior of Low-Aspect-Ratio Reinforced Concrete Shear Walls." ACI Structural Journal, V. 112, No. 5, 2015, pp. 593-604.

[3] Arafa, A., Farghaly, A. S., Benmokrane, B., "Experimental Investigation of GFRP-Reinforced Squat Wall subjected to Lateral Load," 7th International Conference on Advanced Composite Materials in Bridges and Structures (ACMBS-VII), Vancouver, BC, Canada, 2016, 10p.

[4] Oesterle, R. G., Aristizabal-Ochoa, J. D., Fiorato, A. E., Russell, H. G., and Corley, W. G., "Earthquake resistant structural walls—Test of isolated walls—Phase II." Rep. ENV77-15333, National Science Foundation, Arlington, VA, 1979.

[5] Hiraishi, H., "Evaluation of shear and flexural deformations of flexural type shear walls." Bull. New Zealand National Soc. Earthquake Eng., V. 17, No. 2, 1984, pp. 135-144.